JOURNAL OF SOLID STATE CHEMISTRY **134,** 158–163 (1997)
ARTICLE NO. SC977567

Structure and Luminescent Properties of $Y_{17.33}(BO_3)_4(B_2O_5)_2O_{16}$

J. H. Lin, S. Zhou, L. Q. Yang, G. Q. Yao, and M. Z. Su

State Key Laboratory of Rare Earth Materials Chemistry and Applications, Department of Materials Chemistry, Peking University, Beijing 100871, People's Republic of China

and

L. P. You

Laboratory of Electron Microscopy, Peking University, Beijing 100871, People's Republic of China

Received March 14, 1997; in revised form July 21, 1997; accepted July 24, 1997

Yttrium borate $Y_{17.33}(BO_3)_4(B_2O_5)_2O_{16}$, known as Y_3BO_6 previously, was prepared from stoichiometric starting materials of H_3BO_3 and Y_2O_3 by a solid-state reaction at high temperatures. $Y_{17.33}(BO_3)_4(B_2O_5)_2O_{16}$ crystallizes in the monoclinic space group *Cm* with the lattice constants $a = 1816.62(3)$, $b = 365.16(1)$, $c = 1397.75(3)$ pm, and $\beta = 119.75(2)^\circ$. The structure of $Y_{17.33}(BO_3)_4(B_2O_5)_2O_{16}$ was determined using the direct methods applied to X-ray powder diffraction data and consists of BO_3^{3-} and $B_2O_5^{4-}$ borate groups and seven- and eight-coordinated yttrium atoms. The composition obtained from the structure determination corresponds to Y_3BO_6 with a slight excess of B_2O_3. The luminescent properties of the Eu^{3+} doped $Y_{17.33}(BO_3)_4(B_2O_5)_2O_{16}$ materials were studied and the Eu^{3+} emission appears as superimposed bands with a high self-quenching concentration. © 1997 Academic Press

1. INTRODUCTION

It has been known that rare-earth borates of the composition Ln_3BO_6 crystallize in three different monoclinic structures (1) as *Ln* varies from La to Lu. Bartram (2) determined the space groups of these compounds by Weissenberg techniques and refined the lattice constants from X-ray powder diffraction patterns. The compounds were reported to crystallize in three different space groups, i.e., $P2_1/c$ for Ln = La to Nd and $C2/m$, $C2$, or Cm for Ln = Pm to Yb. The lutetium compound adopts the same space group as that of Ln = Pm to Yb, but with a different unit cell. The composition of these compounds was established by phase analysis only and was considered to be the most rare-earth cation-rich phases in Ln_2O_3–B_2O_3 systems. The low symmetry of the structure and the high content of the rare-earth element in these materials stimulated a considerable interest because of their potential uses as hosts for luminescent materials, particularly as X-ray or γ-ray image phosphors (3, 4).

Our initial interest in these compounds was to develop a red emission phosphor under high intense X-ray excitation. During the synthesis process it became evident that the composition of these compounds is not Ln_3BO_6 as previously proposed. When the stoichiometry Ln_3BO_6 was used in the synthesis, the products obtained always contained considerable amounts of $LaBO_3$ or Y_2O_3 in the lanthanum and yttrium systems, respectively. In order to understand the chemical and physical behavior, we decided to investigate the crystal structures of these compounds. The crystal structure of the lanthanum compound was determined using single-crystal techniques (5) and a composition of $La_{26}(BO_3)_8O_{27}$ was obtained from the structure analysis. A comparison of the X-ray powder diffraction patterns between $La_{26}(BO_3)_8O_{27}$ and La_3BO_6 (6) confirmed that $La_{26}(BO_3)_8O_{27}$ is the only binary phase in this composition range. In terms of the composition, this compound can be described as $8La_3BO_6 \cdot La_2O_3$; i.e., the composition is shifted from the La_3BO_6 to the La_2O_3 side in the La_2O_3–B_2O_3 system.

Unlike the lanthanum system, the synthesis of the yttrium compound, Y_3BO_6, always leads to the presence of Y_2O_3 in the products. This phenomenon has also been observed previously by Levin *et al.* (1) and was attributed to the incompleteness of the solid-state reaction. To examine this idea, the reaction was carried out at 1450°C for several days for the yttrium system, but it did not improve the purity of the product. In this paper we report the structure analysis of the yttrium compound by X-ray powder diffraction techniques and demonstrate that the presence of the impurity phase originates from the incorrect assignment of the composition, rather than the incompleteness of the reaction. Starting from the right composition, the yttrium compound can be obtained as a single phase formed at temperatures as

0022-4596/97 $25.00

low as 1150°C. The luminescent properties of the Eu^{3+}-doped yttrium compound are also presented.

2. EXPERIMENTAL

Polycrystalline samples of the yttrium borate were prepared from Y_2O_3 of $> 99.99\%$ purity and analytical grade H_3BO_3 as starting materials. After preheating at 850°C for 6 h, the samples were ground and reheated at temperatures in the range 1150 to 1350°C for 8 h in air. In order to obtain a single-phase product and determine the approximate composition of this yttrium borate, a series of samples with a B/Y ratio varying from 2/9 to 5/9 was synthesized. Three different phases, i.e., the desired phase, Y_2O_3, and YBO_3, were identified. When the B/Y ratio is smaller than 4/9, Y_2O_3 is observed together with the desired phase of the yttrium borate. B/Y ratios larger than 4/9 result in the presence of YBO_3. The sample with B/Y = 4/9 (0.444) was obtained almost phase pure at temperatures as low as 1150°C, indicating that the B/Y ratio of the yttrium compound should be very close to this ratio. The B/Y ratio obtained in the subsequent structure analysis was 0.462. An attempt to grow single crystals by annealing the sample at 1450°C was not successful. The Eu^{3+}-doped luminescent materials were prepared in a similar fashion with Eu_2O_3 as the dopant. About 5 at.% of Li_2CO_3 was used as a flux in the synthesis of the luminescent materials.

The X-ray powder diffraction measurements were carried out on a Rigaku D/MAX-2000 diffractometer using Cu$K\alpha$ radiation from a rotational anode, and the electron diffraction studies were made using a Hitachi H-9000 electron microscope. The infrared spectrum was measured with a Nicolet Magna 750 FT–IR spectrometer. The Raman spectrum was recorded with a Nicolet FT-Raman 910 spectrometer. The fluoroscence spectra were obtained using a Hitachi M-850 fluorescent spectrophotometer, and the decay times were measured with a multiple-frequency fluorophotometer.

3. STRUCTURE DETERMINATION

Due to the lack of suitable single crystals, the crystal structure of $Y_{17.33}(BO_3)_4(B_2O_5)_2O_{16}$ was determined using X-ray powder diffraction techniques. The X-ray powder diffraction data were collected in a 2θ range of 10° to 110°. The crystal system and the unit cell were reexamined using electron diffraction and refined from the powder diffraction pattern using the program FINAX. Figure 1 shows the electron diffraction along [0 1 0], and the systematic absence of the reflections with $h \neq 2n$ is evidenced. From the electron and X-ray powder diffraction patterns, it is confirmed that the yttrium compound crystallizes in a *C*-centered monoclinic structure in one of the space groups *C*2/*m*, *C*2, or *Cm*. The refined lattice constants are $a = 1816.62(3)$, $b = 365.16(1)$, $c = 1397.75(3)$ pm, and $\beta = 119.75(2)°$.

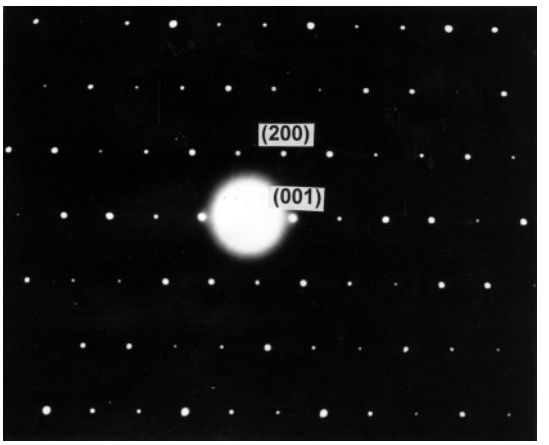

FIG. 1. Electron diffraction of $Y_{17.33}(BO_3)_4(B_2O_5)_2O_{16}$ along [0 1 0].

In order to establish the structure model of the yttrium compound, a full-pattern decomposition program EXTRA (7) was used to extract integrated intensities from the powder pattern. By refining the lattice constants, the background and the profile parameters, a total of 410 individual reflection intensities (164 nonoverlapping) were obtained in a 2θ range from 12° to 90°. The diffraction pattern for $2\theta > 90°$ was not used during the structure model construction, because of the wide overlap of the reflections. The profile refinement lead to a residue value of $R_p = 0.071$.

All of the three possible space groups, *C*2/*m*, *C*2, and *Cm*, were employed in calculations of the structure model. During the structure analysis it was revealed that the presence of the twofold axis resulted in an unrealistic geometry of the polyborate group and the *Cm* space group was, therefore, chosen for this structure. The structure was solved in stepwise fashion by direct methods with the program SIRPOW 92 (8). Initially, the original integrated intensity data were used to locate the heavier atoms. Nine crystallographically independent yttrium positions were recognized from the E-map. The phase information of these yttrium atoms was then used to modify the integrated intensity of the overlapping reflections and 19 oxygen atoms and 1 boron atom were recovered using the renormalized data. The remaining boron atoms were identified by considering the geometrical feature of the borate groups, which were then inserted into the structure model manually. The complete structure was refined with the Rietveld technique. At the initial stage of the refinements, the atoms within the borate groups were constrained. During the refinement it became clear that some of the yttrium positions were not fully occupied. The occupation factors of the yttrium atoms were then refined in subsequent calculations, which resulted in a composition close to $Y_{17.33}(BO_3)_4(B_2O_5)_2O_{16}$. The final composition

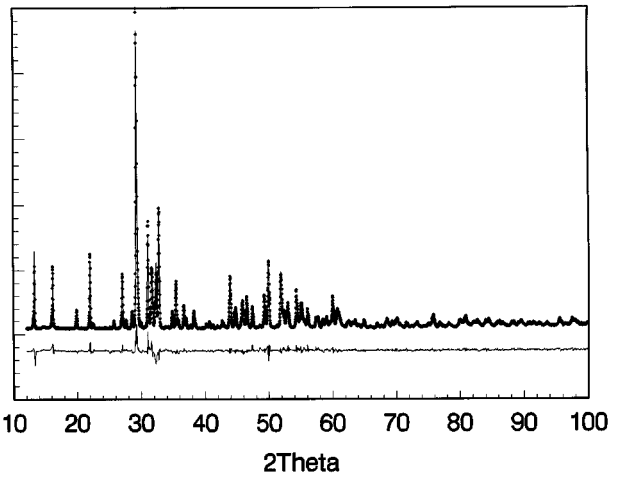

FIG. 2. Refined X-ray powder diffraction patterns of $Y_{17.33}(BO_3)_4(B_2O_5)_2O_{16}$.

was derived by considering both the structure refinement and the charge requirement. Because of the large difference of the atomic scattering powers in the compound, the occupation and temperature factors of the oxygen and boron atoms were constrained as unique values during the refinement. The final residues of the refinement are $R_p = 0.058$ and $R_{wp} = 0.079$. In Fig. 2 we show the refined X-ray powder pattern. The structural parameters are given in Tables 1–3.

TABLE 1
Crystal Data and Structure Refinement for $Y_{17.33}(BO_3)_4(B_2O_5)_2O_{16}$

Molecular formula	$Y_{17.33}B_8O_{38}$
Formula weight	2235.47
Crystal system	Monoclinic
Space group	*Cm* (No. 8)
Unit-cell dimensions (pm)	$a = 1816.62(3)$, $b = 365.16(1)$, $c = 1397.75(3)$, $\beta = 119.75(2)^\circ$
Volume ($\times 10^8$ pm^3)	8.0493(1)
Z	1
Density (Mg m^{-3})	4.611
Color	Colorless
Data collection	
Diffractometer used	D/Max 2000
Monochromator	Graphite
Temperature	293 K
Radiation	Cu$K\alpha$
2θ range for data collection	10° to 110°
Data extraction	
Program used	EXTRA
Profile function	Pseudo-Voigt
2θ range for extraction	12° to 98°
Reflections extracted	410
Independent reflections	164
Structure determination	
Solution	Direct method
System used	SIRPOW 92
Refinement	Rietveld method
Program used	FULLPROF
Final R indices	$R_p = 0.058$, $R_{wp} = 0.079$, $R_B = 0.071$

TABLE 2
Atomic Coordinates and Occupation Parameters for $Y_{17.33}(BO_3)_4(B_2O_5)_2O_{16}$

Atom	x	y	z	f_{occ}
O1	0.000	0	0.000	1.0
O2	0.041(6)	0	0.339(9)	1.0
Y1	0.046(1)	0	0.185(1)	0.848(7)
O3	0.097(5)	0	0.684(9)	1.0
B1	0.129(19)	0	0.403(22)	1.0
O4	0.165(6)	0	0.515(10)	1.0
O5	0.172(4)	0	0.028(9)	1.0
Y2	0.177(1)	0	0.871(1)	0.940(6)
O6	0.177(6)	0	0.354(10)	1.0
B2	0.247(15)	0	0.123(18)	1.0
O7	0.248(5)	0	0.224(10)	1.0
Y3	0.308(1)	0	0.612(1)	1.0
O8	0.322(5)	0	0.124(8)	1.0
O9	0.334(6)	0	0.963(10)	1.0
O10	0.860(4)	0	0.682(9)	1.0
B3	0.371(16)	0	0.076(20)	1.0
O11	0.429(6)	0	0.823(8)	1.0
Y4	0.438(1)	0	0.327(1)	0.884(8)
O12	0.438(6)	0	0.659(9)	1.0
O13	0.458(6)	0	0.139(9)	1.0
B4	0.477(18)	0	0.772(21)	1.0
O14	0.512(5)	0	0.509(7)	1.0
O15	0.564(6)	0	0.833(10)	1.0
Y5	0.570(1)	0	0.001(1)	1.0
O16	0.617(5)	0	0.179(8)	1.0
Y6	0.649(1)	0	0.642(1)	0.918(8)
O17	0.726(5)	0	0.832(8)	1.0
Y7	0.748(1)	0	0.326(1)	0.932(6)
O19	0.820(4)	0	0.507(7)	1.0
O18	0.783(5)	0	0.213(9)	1.0
Y8	0.864(1)	0	0.875(1)	1.0
Y9	0.963(1)	0	0.555(1)	0.910(6)

Note. The equivalent isotropic displacement parameters were refined with unique values for yttrium, oxygen, and boron atoms, respectively (pm$^2 \times 10^{-1}$), $U_{eq}(Y) = 11(4)$, $U_{eq}(O) = 23(7)$, and $U_{eq}(B) = 21(9)$.

4. RESULTS AND DISCUSSION

4.1. Structure of $Y_{17.33}(BO_3)_4(B_2O_5)_2O_{16}$

The asymmetric unit of $Y_{17.33}(BO_3)_4(B_2O_5)_2O_{16}$ consists of 9 yttrium, 19 oxygen, and 4 boron atoms. All atoms are located on the special Wyckoff position 2*a* (x, 0, z), i.e., on the mirror planes at $y = 0$ and 1/2. Figure 3 shows the crystal structure of $Y_{17.33}(BO_3)_4(B_2O_5)_2O_{16}$ along a direction very close to the **b** axis. In contrast to the lanthanum compound $La_{26}(BO_3)_8O_{27}$ (5), the structure of the yttrium compound contains two different kinds of triangular borate groups, BO_3^{3-} and $B_2O_5^{4-}$. The presence of the polyborate

TABLE 3
Interatomic Distances in $Y_{17.33}(BO_3)_4(B_2O_5)_2O_{16}$ Given in pm

Y1–O16	225(6) × 2	Y2-O17	222(6) × 2
Y1–O1	205(3)	Y2–O3	234(6)
Y1–O13	227(6) × 2	Y2–O5	222(7)
Y1–O2	206(6)	Y2–O9	261(7)
Y1–O6	239(7)	Y2–O15	257(6) × 2
Y3–O19	241(6) × 2	Y4–O14	218(8)
Y3–O18	224(7) × 2	Y4–O10	213(8)
Y3–O12	214(8) × 2	Y4–O8	248(7)
Y3–O11	265(6)	Y4–O7	287(7)
		Y4–O13	288(7)
		Y4–O2	271(7) × 2
Y5–O16	214(8)	Y6–O14	235(7)
Y5–O1	230(3) × 2	Y6–O17	225(6)
Y5–O5	256(7) × 2	Y6–O3	220(7) × 2
Y5–O11	257(6)	Y6–O18	224(9)
Y5–O15	235(7) × 2	Y6–O4	279(7) × 2
Y7–O19	232(7)	Y8–O1	229(3)
Y7–O16	233(9)	Y8–O17	233(6)
Y7–O8 10	253(6) × 2	Y8–O18	232(7)
Y7–O7	233(6) × 2	Y8–O9	236(6) × 2
Y7–O9	229(7) × 2	Y8–O11	249(6) × 2
Y9–O14	224(7)	Y9–O10	272(6) × 2
Y9–O19	223(8)	Y9–O12	249(7) × 2
Y9–O3	216(7)		

group results in a higher borate content in the yttrium compound than in the lanthanum compound. The bridged B–O–B angles in the $B_2O_5^{4-}$ group are about 150° and agree with that observed in other borates, such as $Co_2B_2O_5$ (9). If the space group $C2/m$ or $C2$ is chosen, the bridged oxygen atom will be located on the twofold axis and results in a B–O–B angle of 180°, which is not a reasonable geometry for this polyborate anion.

The existence of the BO_3^{3-} and $B_2O_5^{4-}$ borate groups in the structure is supported by Raman and IR spectroscopy. In Fig. 4 we show the Raman and IR spectra of the yttrium compound at room temperature. The IR absorption and Raman peaks at wavenumbers smaller than 500 cm^{-1} originate mainly from the lattice dynamic modes and will not be considered because of their complexity. The vibration modes for the remaining peaks are complicated by the possible overlap of the different borate groups and only those vibration modes which can be attributed to the existence of the borate groups are considered. The assignments of the IR and Raman peaks to the vibration modes of BO_3^{3-} and $B_2O_5^{4-}$ groups were derived by comparison with those of $LaBO_3$ and $Mg_2B_2O_5$ (10), which are illustrated in Table 4. A broad infrared absorption band at around 854 cm^{-1} can be attributed to a stretching mode of B–O–B in $B_2O_5^{4-}$ groups. In the Raman spectrum, two isolated peaks with the Raman shifts around 926 and 1056 cm^{-1} are associated with ν_s of BO_3^{3-} and ν_s of BO_2 in $B_2O_5^{4-}$ groups,

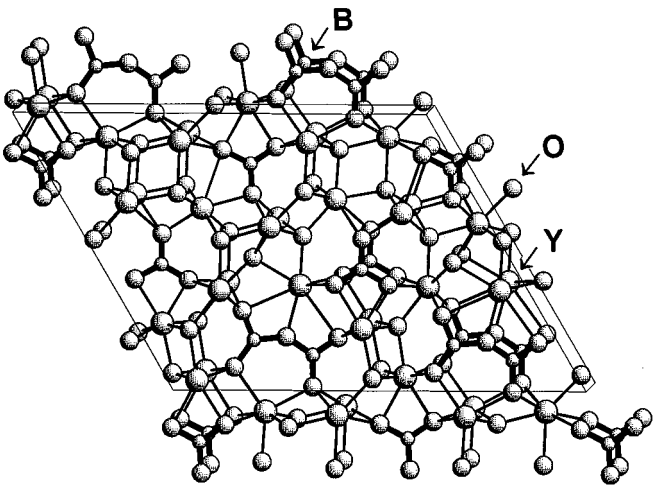

FIG. 3. Crystal structure of $Y_{17.33}(BO_3)_4(B_2O_5)_2O_{16}$ projected along a direction close to the **b** axis.

respectively. These characteristic peaks may represent the existence of two different borate groups in the structure.

The structure of the yttrium compound $Y_{17.33}(BO_3)_4(B_2O_5)_2O_{16}$ is different form that of the lanthanum compound $La_{26}(BO_3)_8O_{27}$, not only because of the presence of the polyborate group $B_2O_5^{4-}$, but also because of a different packing of the atoms. In $La_{26}(BO_3)_8O_{27}$ the lanthanum and oxygen atoms form a fluorite-type lattice, and the presence of the boron atoms causes a square antiprismatic distortion at some of the lanthanum positions (5). In contrast, the atoms in the structure of $Y_{17.33}(BO_3)_4(B_2O_5)_2O_{16}$ seem to be packed more efficiently than in the fluorite-structure type. The coordination polyhedra of the yttrium atoms are all irregular with seven- or eight-coordinated oxygen atoms. Interestingly, most of the yttrium coordination polyhedra (six in nine) in the structure are very similar to that observed in *A*-type rare-earth sesquioxides Ln_2O_3 (11). In Fig. 5 a typical coordination polyhedron of the

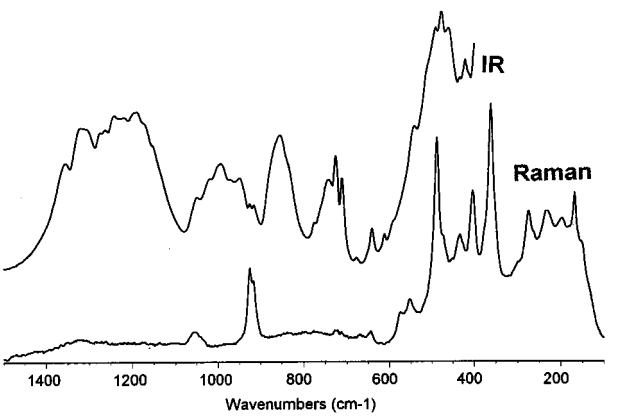

FIG. 4. IR and Raman spectra of $Y_{17.33}(BO_3)_4(B_2O_5)_2O_{16}$.

TABLE 4
The Assignments of IR and Raman Spectra for $Y_{17.33}(BO_3)_4(B_2O_5)_2O_{16}$

IR absorption (cm^{-1})	Raman shifts (cm^{-1})	Possible assignments
1355		νBO
1320		
1241		ν_{as} BO_3^{3-}
1220		ν_s BO_2
1191		
1048	1056	ν_s BO_2 in $B_2O_5^{4-}$
994		
949	925	ν_a BO_3^{3-}
854		ν_s BOB
742	728	γBO_3^{3-} and γBO_2
725		
710		

yttrium atom is presented, together with that in *A*-type Ln_2O_3 for comparison. This seven-coordinated polyhedron can be considered as a monocapped octahedron. It is known that the rare-earth sesquioxides crystallize in three different structure types, namely *A*-, *B*-, and *C*-type. According to the phase diagram (11), the *A*-type structure is favored for the light rare earth. The heavy rare-earth elements, on the other hand, crystallize in the *C*-type structure, which is a defect fluorite structure. The *B*-type structure, as a distorted version of the *A*-type structure, preferentially appears in the middle range of the rare-earth series. The coordination preference of the rare-earth ions seems to be reversed in these borate compounds. For the light rare-earth elements from La to Nd, the borate compounds crystallize in the $La_{26}(BO_3)_8O_{27}$ structure, in which the lanthanum atoms are coordinated by cubic or square antiprismatic polyhedra. The borate compounds of the heavier rare-earth elements Sm to Yb crystallize in the $Y_{17.33}(BO_3)_4(B_2O_5)_2O_{16}$ structure, mainly with monocapped octahedra. This coordination preference needs to be further verified by a structure determination of the lutetium compound, which is the last unknown structure in the series.

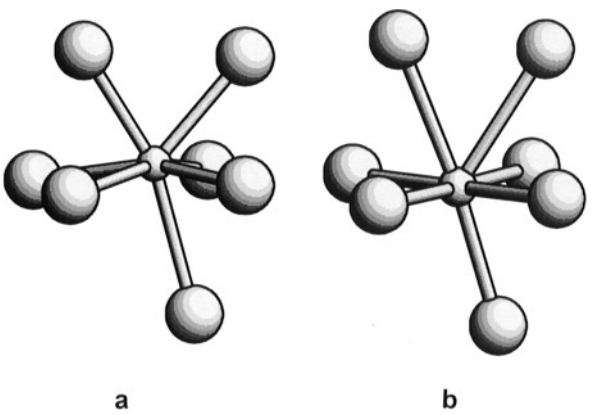

FIG. 5. A typical coordination polyhedron of yttrium atoms in (a) *A*-type rare-earth sesquioxide and (b) $Y_{17.33}(BO_3)_4(B_2O_5)_2O_{16}$.

Although the refinement of the structure is quite satisfactory as far as the residue ($R_p = 0.058$) is concerned, there are a number of uncertainties regarding the bond distances between the yttrium and oxygen atoms, because some Y–O bond distances are slightly smaller than the sum of the ionic radii (232 pm). The deviation in the bond distances may originate from the difficulty to precisely locate the oxygen atoms in the presence of many heavy atoms, as well as in the limitation of the powder diffraction techniques. Nevertheless, the structure analysis provides a reasonable structure model for this "*old*" yttrium borate and, with this structure model, many observations in the synthesis and physical properties can be explained.

4.2. Luminescent Properties

The europium borate adopts the same structure as the yttrium compound (1) and the ionic radii of Eu^{3+} and Y^{3+} are very similar; therefore, a large solubility of europium atoms in the yttrium borate can be expected. We have dissolved up to 20 at.% of europium in $Y_{17.33}(BO_3)_4(B_2O_5)_2O_{16}$, without any other phases being observed in X-ray diffraction patterns. Considering the difference in scattering factors of europium and yttrium, the distribution of the dissolved europium atoms in yttrium borate should be distinguishable by the Rietveld refinement. Two typical solid solution samples, $(Y_{0.95}Eu_{0.05})_{17.33}(BO_3)_4(B_2O_5)_2O_{16}$ and $(Y_{0.75}Eu_{0.25})_{17.33}(BO_3)_4(B_2O_5)_2O_{16}$ were employed for the refinement. During the refinement only the occupation factors of the yttrium atoms were varied which resulted in an almost random distribution of europium in all of the nine crystallographically independent yttrium positions.

The excitation and emission spectra of Eu^{3+}-doped $Y_{17.33}(BO_3)_4(B_2O_5)_2O_{16}$ are shown in Fig. 6. The excitation spectrum consists of a broad band at about 270 nm and several sharp peaks at longer wavelengths. The broad band originates from the charge transfer excitation from the Eu^{3+} nearest-neighbor oxygen atoms. The sharp excitation peaks correspond to the transitions within the f^6 configuration. The emission spectrum contains several peaks ranging from 580 to 720 nm and are attributed to the optical transitions from the excited $^5D_0$ level to the ^7F_J ($J = 1$ to 6) levels of the f^6 configuration. The yttrium positions in the structure have no inversion symmetry and because of the mixing of opposite-parity states into the $4f^6$ configuration, the forced electric–dipole transition is allowed. The $^5D_0$–$^7F_2$ transition is a typical symmetry-sensitive transition and can be expected to dominate in the emission spectrum. This agrees with experimental results, as shown in Fig. 6.

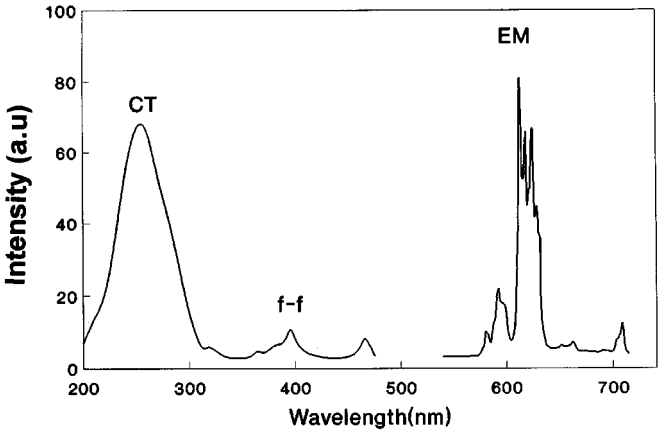

FIG. 6. Emission and excitation spectra of $Y_{17.33}(BO_3)_4(B_2O_5)_2O_{16}$: Eu^{3+}.

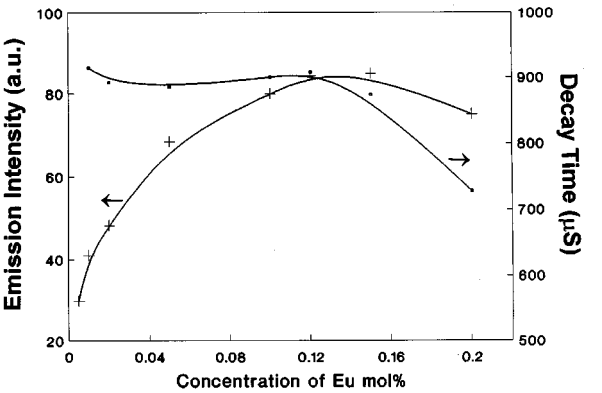

FIG. 7. Concentration dependence of Eu^{3+} emission intensity and decay time of $Y_{17.33}(BO_3)_4(B_2O_5)_2O_{16}:Eu^{3+}$.

The emission of single Eu^{3+} atoms should appear as sharp lines in solids. However, there are nine crystallographically independent yttrium positions in the $Y_{17.33}(BO_3)_4(B_2O_5)_2O_{16}$ structure, and furthermore, the doped europium atoms are randomly distributed in all of these positions. Since the crystal field and the site symmetry are different, the Eu^{3+} emission peaks may vary slightly from one position to the other. The observed emission spectrum is a superposition of Eu^{3+} optical transitions from all individual positions and the peaks therefore appear wider than normal.

The concentration dependence of the Eu^{3+} emission intensities is illustrated in Fig. 7. The emission intensities increase with the doping concentration up to about $C_{Eu} = 15\%$ and then decline slightly. The energy migration between the rare-earth ions in these materials is high because of the large spectral overlap (12). In many host materials, the concentration quenching becomes efficient for doping concentrations of a few percent. In this material, however, the energy transfer between the Eu^{3+} ions is not efficient, resulting in an unusually high quenching concentration. The decay times of the Eu^{3+} emission, measured with the phase-modulation method, as shown in Fig. 7. The decay times remain almost constant at low Eu^{3+} concentration. A significant decrease of the decay time is observed at doping concentrations $C_{Eu} > 15\%$. If we consider $C_{Eu} = 20\%$ to be the critical concentration the approximate critical energy transfer distance can be calculated to be 3.8 Å. Such a short critical distance of the energy transfer indicates that the energy transfer between Eu^{3+} in this material is probably due to exchange interactions.

ACKNOWLEDGMENTS

The financial support for this work was received from the National Natural Science Foundation of China and the State Science and Technology Commission of China.

REFERENCES

1. E. M. Levin, C. R. Robbins, and J. L. Warring, *J. Am. Ceram. Soc.* **44,** 87 (1961).
2. S. F. Bartram, "Proc. 3rd Conf. Rare Earth Res., Clearwater, FL, 1963," N.S.A 17, No. 32035, pp. 165/80, 1964.
3. F. Y. Guo, N. H. Liu, and Z. F. Song, *J. Chinese Rare Earth Soc.* **9,** 319 (1991).
4. Y. A. Peng, Q. H. Li, J. H. Lin, and F. Y. Guo, *J. Rare Earth* (Eng.) **13,** 261 (1995).
5. J. H. Lin, M. Z. Su, K. Wurst, and E. Schweda, *J. Solid State Chem.* **126,** 287 (1996).
6. J. H. Lin, E. Schweda, F. Y. Guo, and M. Z. Su, *J. Rare Earth* (Special Issue) 234 (1995).
7. A. Altomare, M. C. Burla, G. Cascarano, C. Giacovazzo, A. Guagliardi, A. G. G. Moliterni, and G. Polidori, *J. Appl. Crystallogr.* **28,** 842 (1995).
8. A. Altomare, G. Cascarano, C. Giacovazzo, A. Guagliardi, M. C. Burla, G. Polidori, and M. Camalli, "SIRPOW 92 User's Manual."
9. Y. Takeuchi, *Acta Crystallogr.* **5,** 574 (1952).
10. Von W. Bues, G. Foester, and R. Schmitt, *Z. Anorg. Allg. Chem.* **344,** 148 (1966).
11. E. Schweda, *Key Eng. Mater.* **68,** 187 (1992).
12. G. Blasse and B. C. Grabmaier, "Luminescent Materials," p. 96. Springer-Verlag, Berlin, New York, 1994.